Catalysis Science & Technology

Accepted Manuscript

ROYAL SOCIETY OF CHEMISTRY

www.rsc.org/catalysis

Journal Name

ARTICLE

Towards efficient catalysts for the oxidative dehydrogenation of propane in the presence of CO_2: Cr/SiO_2 systems prepared by direct hydrothermal synthesis

Received 00th January 20xx,
Accepted 00th January 20xx

DOI: 10.1039/x0xx00000x

www.rsc.org/

M.A.Botavina [a], Yu.A.Agafonov [b], N.A.Gaidai [b], E.Groppo [a], V. Cortés Corberán[c], A.L.Lapidus [b]and G.Martra [a†]

Cr/SiO_2 catalysts (Cr loading in the 0.25-2.0 wt% range) have been prepared by direct hydrothermal synthesis in the presence of templating agents, in order to attain porous systems with high specific surface area (in the 600-1000 $m^2 \cdot g^{-1}$ range), and then characterized and tested in the oxidative dehydrogenation of propane in the presence of CO_2 or CO_2+O_2 as oxidant. The extent and regularity of mesopores decreased significantly by increasing the Cr content (X-ray diffraction, N_2 adsorption, transmission electron microscopy), but this did not limit the catalytic performances of the catalysts with higher Cr loadings. In all cases the only chromium species found were surface chromates (diffuse reflectance electronic spectroscopy and X-ray absorption near edge spectroscopy), accompanied by Brønsted acid centres (infra-red spectra of adsorbed NH_3). All catalysts appeared stable towards irreversible deactivation, even after ca. 900 min of testing, and yields in propene as high as 40% were attained. The combination of spectroscopic and catalytic results allowed to rationalize, at least in part, the role of different oxidants in defining the chromium oxidation state and a tentative correlation of the oxidation state of Cr species during the reaction (Cr^{2+}/Cr^{3+}) with selectivity in propene is suggested.

1. Introduction

Propene (C_3H_6) is among the foundation feedstock for large volume commodities and specialty chemicals, such as cumene, acrylonitrile, propylene oxide and high-purity polypropylene, and its demand is expected to increase significantly in the near future.[1] At present, its industrial production is based on non-oxidative processing of petroleum-based materials, via steam cracking, fluid-catalytic-cracking and catalytic dehydrogenation.[2] As far as the catalytic dehydrogenation is concerned, commercial processes use Cr_2O_3/Al_2O_3 (18-20 Cr wt%; Catofin press) or Pt(<1 wt%),Sn (1-2 wt%)/Al_2O_3 (Oleflex process).[3] Possible replacements with lower costs and sustainable alternatives is attracting a rising interest since many years, and the oxidative dehydrogenation (ODH) of propane appeared among the most promising, because of the higher energy efficiency (ODH is exothermic, while dehydrogenation and cracking are endothermic processes), and process simplicity. A review on the catalysts for propane ODH was compiled by Cavani et al. in 2007,[2] who considered the performances in ODH of propane with O_2 as oxidant of almost 100 catalysts, with different active phases, reported in literature over the 2000-2006 period, and concluded that the best propylene yields resulting from propane ODH (ca. 30%) were still far from being interesting for industrial implementation, as well as the information concerning catalyst lifetime appeared quite limited. Moreover, in that review the set-up of catalytic materials and/or reactor configurations capable of maintaining high selectivity to propylene under conditions leading to high propane conversion was addressed as main direction for future development. Later on, an initial yield in C_3H_6 as high as ca. 47%, decreasing to ca. 33% after 8 h on stream were reported for propane dehydrogenation over GaO_x based catalysts.[4] More recently, the kinetics for the ODH of C_3H_8 on VO_x catalysts was reviewed by Carrero et al., and for the systems considered the combination of reported conversions and selectivities resulted in yields in C_3H_6 not exceeding 30%.[5] Conversely, Ovsitser et al., reported the attainment of a yield in propene of ca. 40% for the oxidative dehydrogenation of C_3H_8 under O_2 lean-conditions over VO_x/SiO_2 catalysts, even a quite long reaction time.[6] Similar results were obtained by these authors for the oxydative dehydrogenation of iso-C_4H_{10} to iso-C_4H_8.[7]

In this respect, the attainment of high selectivity to olefins via ODH of alkanes is basically limited, from a chemical point of view, by the use of O_2 as oxidant, because of the occurrence of the over-oxidation to carbon oxides of both fed paraffins and produced olefins. On such a basis, the use of CO_2 as mild oxidant has attracted attention after the successful use in other partial oxidation reactions such as dry reforming[8,9] and oxidative coupling of methane.[10, 11] Although ODH of propane in the presence of CO_2 is an endothermic process (ΔH_{298K}= + 166.6 kJ/mol), the addition of a small amount of oxygen can turn the process towards an exothermic character, and additional positive effects towards the catalyst coking might be expected.

[a] Department of Chemistry and "Nanostructured Interfaces and Surfaces - NIS" Interdepartmental Centre , via P.Giuria, 7, 10125, Torino, University of Torino, Italy.
[b] N.D. Zelinsky Institute of Organic Chemistry, Russ.Acad.Sci., Leninskii pr, 47, 117991 Moscow, Russia.
[c] Institute of Catalysis and Petroleumchemistry, CSIC, Calle Marie Curie 2, 28049 Madrid, Spain.
† Corresponding author; phone: +39 - 011 6707538, FAX: +39 - 011 6707855, e-mail: gianmario.martra@unito.it

Among the heterogeneous catalysts tested in processes involving CO_2 as oxidant, materials based on chromium supported on silica exhibited the most promising performances.[12-19] Thus, in a previous study we investigated the performances of a series of CrO_x/SiO_2 catalysts in the ODH of propane carried out in a regime of high conversion (≥40%), similar to that required in industrial processes.[20] Satisfactory results were obtained for the material with a 5.00 wt% chromium loading that, however, suffered an irreversible deactivation due to the agglomeration of surface chromium species. To overcome this problem, we turned our interest towards the dispersion of chromium species on high specific surface area silicas, typically of the mesoporous type, via a direct hydrothermal synthesis (DHS) in the presence of structure directing agents, as reported in the literature.[18, 19, 21-28] Wang et al. [18] provided evidence for the resistance to the irreversible deactivation of Cr/MCM-41 catalysts (3.4 wt% Cr) during the ODH of C_3H_8 with O_2, but in reaction conditions resulting in a C_3H_8 conversion of ca. 30% at maximum and propene yield of 26%, and the stability of the catalyst was followed over a period not longer than 300 min.

Here, we report the results of a physical-chemical characterization and catalytic testing of a series of Cr/SiO_2 materials prepared by DHS (Cr loadings in the 0.25 - 2.00 wt% range) targeting ODH conditions (using both CO_2 and a CO_2+O_2 mixture as oxidants) as closest as possible to industrial applications.

2. Experimental

2.1. Catalyst preparation and treatments

The investigated materials were prepared by direct hydrothermal synthesis, following the protocol usually employed to obtain mesoporous structures of the MCM-41 type.[18] Cetyltrimethylammonium bromide (Sigma-Aldrich), pure fumed silica (Aerosil 300, Degussa) and chromium nitrate (Sigma-Aldrich) were used as structure directing agent, silica and chromium source, respectively. Tetramethylammonium hydroxide (Sigma-Aldrich) was used to maintain a pH of ca. 11.0. The relative amount of $Cr(NO_3)_3$ varied among the series of preparations, in order to attain chromium loadings ranging from 0.25 to 2.00 wt%. For the sake of comparison, also bare MCM-41 silica was prepared. Moreover catalysts with Cr loadings 3.00 and 5.50 wt% were prepared. However, in preliminary tests they exhibited a slightly lower catalytic activity than the catalyst with 2.00 wt% Cr content (see Electronic Supplementary Information (ESI), Fig. S1), and then they were not longer considered. The synthesis gels were stirred at 308 K (water bath) for 2 h, transferred into a Teflon lined autoclave and kept at 373 K for 48 h. The obtained powder/liquid mixtures were filtered at room temperature and carefully washed with distilled water (three doses of 50 mL). Samples were then dried at 373 K and placed into a gas-flow furnace, where the temperature was raised to 873 K (heating rate: 2 K/min) under flowing N_2 (1 atm, 2 L·min^{-1}). The flow was then switched to O_2 (1 atm, 2 L·min^{-1}) for calcination for 8 h. The final cooling to room temperature occurred under O_2 flow. Codes, chromium content and textural features of the various catalysts are listed in Table 1.

For characterization, fresh catalysts underwent the following treatments:

i) dehydration/dehydroxylation, keeping chromium in the +6 oxidation state: the materials were re-calcined at 873 K (2 h) and subsequently cooled down to r.t. under dry O_2 (1 atm; 2 L/min). Samples treated in such way will be hereafter referred to as "dehydr/ox ". This treatment was also carried out on aliquots of used catalysts (regenerated as reported at the end of section 2.3 “Catalytic tests”) which were analysed by DR UV-Vis-NIR spectroscopy.

ii) Reduction of surface chromium species: a typical protocol for the conversion of Cr^{6+} into Cr^{2+} was followed.[29] Hence, samples were calcined in O_2 (100 Torr) at 873 K for 1h, cooled (in O_2) to 623 K, then treated in CO (40 Torr) and outgassed at the same temperature (30 min each step) and finally cooled to room temperature. The treatment in CO was repeated three times, with intermediate outgassing. Samples treated in such way will be hereafter referred to as "dehydr/red".

Moreover, a catalyst, the 1.0-Cr/DHS one, was treated *in situ* in the cell used for XANES measurements in the presence of the various reaction mixtures. The selection of this catalyst, anyway representative of the series of materials tested (*see below*), resulted from sample availability and Cr content high enough to obtain XANES spectra with a satisfactory signal to noise ratio in the presence of carbonaceous deposits, resulting in a further dilution of Cr content. For these measurements the catalyst was activated at 873 K (2 h) in static O_2 (100 Torr) and then exposed to different reaction mixtures (40 Torr): C_3H_8:N_2=15:85; C_3H_8:CO_2:N_2=15:30:55; C_3H_8:O_2:N_2=15:3:82; C_3H_8:CO_2:O_2:N_2=15:30:3:52 at 873 K for 2h.

2.2. Characterization methods

X-ray diffraction (XRD) patterns were collected by a Philips PW 1850 powder diffractometer (Co Kα radiation, 40 kV with 20mA current) and indexed by using Philips X’pert High score software.

Specific surface areas (SSA) were measured with a Micromeritics ASAP 2010 by nitrogen adsorption at 77 K using the BET model for data analysis, while pore volume and size were calculated by using the BJH model (adsorption branch). Before measurements all samples were outgassed at 473 K to a residual pressure of 1.0×10^{-4} Torr (1 Torr: 133.33 Pa).

Observations and chemical analysis of the samples by transmission *electron microscopy coupled with energy dispersive X-ray spectroscopy* (TEM-EDS) were performed with a JEOL 3010-UHR instrument (acceleration potential of 300 kV) equipped with an Oxford Inca Energy TEM 200 EDS X-rays analyzer. To obtain a good dispersion on the sample holder and avoid any contamination, lacey carbon Cu grids were briefly contacted with the powders, resulting in the adhesion of some particles to the sample holders by electrostatic interactions. Quantitative compositional studies were carried out using the Oxford INCA Microanalysis Suite software. The mean composition resulted from the average of 7 measures in different regions. The Cr Kα emission at 5.4 keV was selected for EDS mapping of this element.

Table 1. Codes, composition and textural properties of the fresh Cr/DHS catalysts. The values of textural features of used/regenerated catalysts are in Table S1 in the ESI

entry	**Catalyst**	Cr loading (wt%)	Specific surface area (m^2/g)	Specific Cr loading (at.Cr/nm^2)	Total pore volume (cm^3/g)	2-3 nm pore volume (cm^3/g)	Pore diameter (nm)	Wall thickness (nm)
1	MCM-41	-	1273	-	0.79	0.74	2.5	0.19
2	0.25-Cr/DHS	0.25	960	0.03	0.56	0.50	2.6	0.15
3	0.5-Cr/DHS	0.5	957	0.06	0.61	0.50	2.7	0.13
4	1.0-Cr/DHS	1.0	910	0.14	0.55	0.42	2.8	-
5	2.0-Cr/DHS	2.0	663	0.35	0.41	0.29	2.9	-
6*	2.0-Cr/DHSc	2.0	493	0.35	0.22	0.11	2.4	-

* Coked sample

Diffuse reflectance (DR) UV-Vis-NIR spectroscopy measurements were performed with a VARIAN Cary 5000 UV-Vis-NIR spectrophotometer, equipped with an integrating sphere coated with Spectralon®. The powders (gently ground in an agate mortar to disrupt agglomerates) were placed in a flow reactor with a side branch equipped with an optical quartz window, where the powders were transferred for the spectroscopic measurements. The spectra, initially collected in reflectance mode, were converted to the Kubelka-Munk (K-M) function. To avoid exceeding the limit of validity of such function (K-M values ≤1) all samples were diluted with the bare MCM-41 silica (ground in a similar way) in a 1:7 ratio by weight. UV-Vis spectroscopy was also employed in the transmission mode for checking the possible presence of chromium in the filtrate when the catalysts were recovered from the powder/liquid synthesis mixtures.

X-ray absorption spectroscopy (XAS) measurements at the Cr K-edge (5989 eV) were performed at the BM23 beamline of the European Synchrotron Radiation Facility (ESRF, Grenoble, France). The white beam was monochromatized using a Si(111) double crystal. Harmonic rejection was performed by using silicon mirrors. Due to Cr dilution, XAS spectra were collected in fluorescence mode, by means of a Vortex detector. The intensity of the incident beam was monitored by an ionization chamber filled with 1 bar of 20% N_2 – 80% He. The beam transmitted through the sample passed further through a second ionization chamber, a Cr foil and a third ionization chamber to ensure the correct energy calibration for any acquisition. The samples were measured in the form of pressed pellets inside the cryostat available on BM23, which is small enough to enter in the glove-box. Pellets of samples treated in different conditions were performed directly inside the glove-box and transferred in the cryostat. Measurements were performed close to liquid He temperature and in dynamic vacuum (pressure lower than 1.0 10^{-6} Torr, 1 Torr: 133.33 Pa) in order to avoid contamination of the samples. XANES spectra were acquired with an energy step of 0.4 eV and an integration time of 2s/point.

Infrared spectra were collected using a Bruker IFS 28 spectrometer (MCT detector; resolution: 4 cm^{-1}). The samples were pressed in self supported pellets and placed in a quartz cell with KBr windows that, once connected to conventional vacuum lines (residual pressure lower than 1.0×10^{-5} Torr), allowed all thermal treatments and adsorption/desorption experiments of ammonia to be carried out in situ. Before IR measurements, the samples were submitted to treatment i) of the previous section (dehydrated and oxidized state). The spectra of adsorbed NH_3 are reported in absorbance mode, having subtracted the spectra of the samples before adsorption as a background. High purity ammonia (Praxair) was used, without any further purification except water trapping at ca. 243 K (cooling medium: solid/liquid ethanol).

Thermogravimetric analyses (TGA) were carried out with TAQ 600 TGA instrument. Samples were heated at a rate of 20 K/min from room temperature to 1073 K under air flow (6L/h).

2.3. Catalytic tests

Catalytic tests were carried out in a flow reactor, under atmospheric pressure. All the tests were conducted at 873 K since non catalytic conversion of C_3H_6 can occur to a slight extent only at T≥923 K, as reported in previous work.[20] A volume space velocity (w) of 200 h^{-1} was adopted to obtain a high propane conversion.

The feed composition was C_3H_8:CO_2:N_2 = 15:30:55 or C_3H_8:CO_2:O_2:N_2 = 15:30:3:52 (in mol%). Initial partial pressures were $P^0_{C3H8} = 0.15$ atm and $P^0_{CO2} = 0.30$ atm (1 atm = 101.33 kPa); the relative amount of O_2 used in the second case was the same as that in our previous work devoted to catalysts prepared by wet impregnation[20]. Prior to tests, all catalysts were activated in air flow at T= 873 K (heating rate: 10 K/min) for at least 1h. The reaction products were analyzed by GC methods (instrumental error: ±4%) using two columns: molecular sieve 5A (H_2, O_2, N_2, CH_4, CO,) and Porapak Q (CO_2, H_2O hydrocarbons). The first analyses, providing data assumed as initial conversion and selectivity, were carried out after 20 min of reaction. After each run, the catalysts were treated in air flow at T= 873 K (heating rate: 10 K/min) for 6h, and then tested in a next run. Yield and selectivity values were calculated on the basis of the concentrations of the gas phase components. Formulae used for the calculation of conversion, selectivity and yield are reported in the ESI.

3. Results and discussion

3.1. Composition, structural and textural features of the catalysts

At the end of the syntheses in autoclave, no chromium was found in the aqueous phases separated by filtration (analyzed by UV-Vis spectroscopy), indicating that the actual Cr content of the catalysts corresponded to the nominal one (Table 1, column 3).

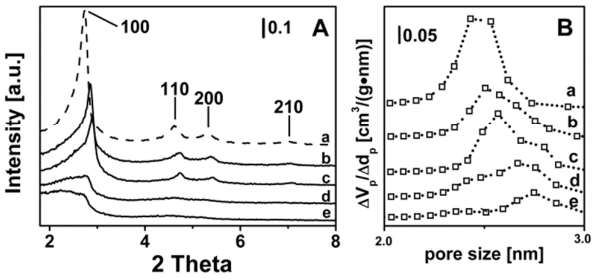

Fig. 1. XRD patterns (Section A) and pore size distribution (Section B) of the as-prepared catalysts: a) pure MCM-41, for the sake of comparison, b) 0.25-Cr/DHS, c) 0.5-Cr/DHS, d) 1.0-Cr/DHS, e) 2.0-Cr/DHS.

XRD patterns (Fig. 1A) typical of regular mesoporous structures of the MCM-41 type, exhibiting (100), (110) and (200) diffraction peaks, were obtained for the bare silica reference material (curve a) and, with some decrease in intensity, for catalysts with Cr loading ≤ 0.5 wt% (curves b, c). Furthermore, in the latter two cases the presence of chromium resulted in a shift of the (100) peak to larger angles, due to a decrease in the pore wall thickness (Table 1, last column). Higher Cr loading resulted in an almost complete vanishing of the MCM-41 structure, and only traces were still present for 2.0–Cr/DHS (Fig. 1, curves d, e). Such trend is in agreement with literature data, although the persistence of MCM-41 mesoporous structure for Cr content of ca. 1.0 wt% was reported [18, 27, 30] and, by keeping the nascent materials under autogenous pressure at ca. 373 K for 8 days, also for Cr content of 6.0 wt%.[25]

The loss of ordered mesoporous structure resulted in a decrease of SSA, of the order of ca. 24-30% for Cr content up to 1 wt%, and of ca. 50% for 2.0-Cr/DHS. As a consequence, the theoretical surface dispersion of Cr ions increase of more than 10 times passing from 0.03 (for 0.25-Cr/DHS) to 0.35 at/nm^2 (2.0-Cr/DHS), which, nevertheless, is still a quite low surface density (Table 1, column 5). As expected, the decrease of SSA was accompanied by a significant decrease of porosity (Table 1, columns 4, and 6, respectively). It is worthwhile to notice that the mesopore size distribution (Fig. 1B) evolved from monomodal for the bare MCM-41 silica (centered at ca. 2.5 nm, curve a), to a bimodal for Cr loadings up to 1.0 wt% (curves b-d), becoming again monomodal for 2.0-Cr/DHS (curve e), but with a larger mean pore size (centered at 2.7 nm). At the same time for all Cr loadings some larger pores (up to 100 nm) were detected, likely due to an interparticle porosity associated to the presence of disordered mesoporous silica phase (will be discussed below).

Such textural evolution was accompanied by parallel changes in structure and morphology observed by TEM. All materials, included the bare MCM-41 silica, appeared constituted by two types of particles, namely large grains with regular porous structure (Fig. 2A), and aggregates of small particles, a fraction of which still exhibits randomly arranged mesopores (Fig. 2B). Grains of the first type were predominant for bare silica, 0.25-Cr/DHS and 0.5-Cr/DHS, i.e. the materials exhibiting a typical MCM-41 XRD pattern, whereas the disordered phase prevailed by far for the remaining 1.0-Cr/DHS and 2.0-Cr/DHS catalysts.

A mapping of the location of Cr was carried out by EDS, and the contours of the obtained maps appeared almost coincident with the borders of the particles aggregates, observed in the corresponding TEM images, independently on the ordered or disordered porous structure (Fig. 3). Nevertheless, the Cr loading measured by EDS on regions with MCM-41 pore structure was, on average, slightly higher than for those with a disordered arrangement of pores (e.g 2.5% ±0.5% wt% and 2.0 ± 0.7% wt% respectively, in the case of the 2.0-Cr/DHS).

XRD, volumetric and TEM/EDS measurements were repeated for the catalysts regenerated after the first catalytic run, and essentially the same results were obtained (see Electronic Supplementary Information (ESI), Table S1 and Fig. S2), demonstrating that neither the textural properties nor the Cr distribution change during the catalytic reaction.

3.2. Nature and structure of supported Cr species

Oxidation and coordination state, as well as the speciation and accessibility of supported chromium species in the whole series of Cr/DHS catalysts were evaluated by DR UV-Vis-NIR spectroscopy and, for the 0.5-Cr/DHS catalyst, also by XANES. The results obtained with both methods on this latter sample are shown in Fig.4 and discussed below, while the electronic spectra of the full series of catalysts are reported in Fig.S4 and S5 in the ESI.

The XANES spectrum of dehydr/ox 0.5-Cr/DHS sample (Fig. 4A, curve a) is very similar to those reported in literature for analogous

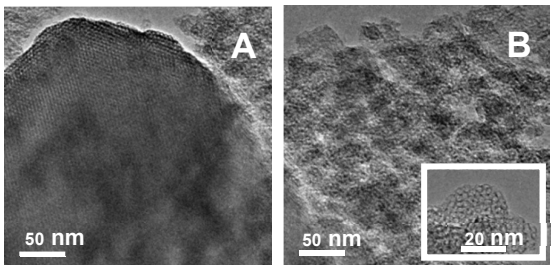

Fig. 2. TEM images of 2.00-Cr/DHS, representative of the size and morphology of the ordered (section A) and disordered (section B) porous phases observed in all samples.

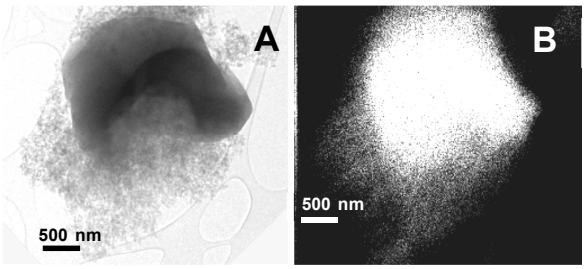

Fig. 3. TEM/EDS data obtained for the 2.0-Cr/DHS sample, representative of all catalysts: image (A) and corresponding EDS map of the Cr location (B) of an aggregate of the ordered and disordered porous phases. The difference in the brightness in the maps are mainly due to differences in thickness of the analysed regions.

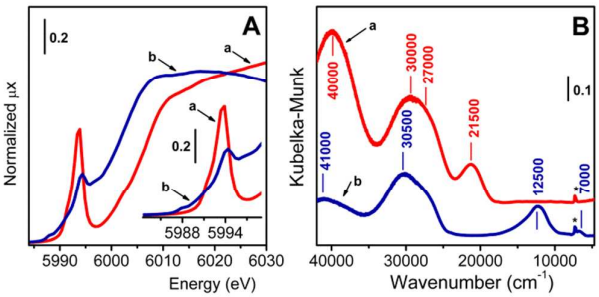

Fig. 4. Normalized XANES (A) and DR UV-Vis (B) spectra of 0.5-Cr/DHS catalyst in the dehydr/ox (curves a, red) and dehydr/red (curves b, blue) states. The insert in part A shows an enlargement of the pre-edge region. In part B, the sharp component labelled with an asterisk is due to the $2\nu_{OH}$ vibration of silanols at the support surface.

Cr^{6+}/SiO_2 catalysts, employed for both propane ODH reactions[16, 18] and ethylene polymerization (Phillips catalyst).[31-36] In particular: i) the edge value, evaluated at the maximum of the derivative curve, is at 6007 eV (i.e. ca. 17 eV lower than Cr foil, consistent with XANES spectra of Cr^{6+} compounds); ii) the intense pre-edge peak centered at 5994 eV (normalized intensity= 0.74, fwhm= 2.1 eV), is characteristic of Cr^{6+} species in a nearly perfect tetrahedral symmetry and assigned to transition of the excited 1s electron to hybrid p–d orbitals of Cr.[24, 31-37]

The corresponding DR UV-Vis-NIR spectrum (Fig. 4B, curve a) exhibits three main components, at ca. 40000, 30000 (with a shoulder at 27000) and 21500 cm^{-1}.

On the basis of the works by Weckhuysen et al.,[36-40] they could be attributed to ligand to metal charge-transfer transitions from oxygen to Cr^{6+} in surface chromate species, ranging from monochromates to polychromates. The two bands at ca. 21500 and 40000 cm^{-1} are not structured enough to recognize specific sub-bands due to chromate species with a different speciation, whilst the components at ca. 27000 cm^{-1} and 30000 cm^{-1} can be attributed to monochromates and di-and/or polychromates, respectively. However, the possibility that these two component might be both due to monochromate species with different local structures cannot be ruled out.[39] As for polychromates, if present, they should account for a minor part of the spectrum, because the high SSA should have favoured a high dispersion of Cr species during the synthesis. Furthermore, their relative amount is expected to increase by increasing the Cr content; conversely, all bands present in the spectrum exhibited a proportional increase in intensity ranging along the whole series of catalysts (see Fig. S3 in the ESI). It is worth noticing that the band at 21500 cm^{-1} is attributed to an oxygen to chromium CT transition involving the double bonded oxygen ligands of chromates; its low wavenumber position makes this band a valuable fingerprint of the presence of chromates.

The possibility that part of chromium species was embedded into the silica matrix during the synthesis, and then not available for the catalytic reaction, should not be excluded a priori. For this reason, catalysts underwent a thermal treatment in the presence of CO (see Experimental), expected to convert to Cr^{2+} all chromium species actually exposed at the surface, leaving untouched those embedded within the silica framework, if any. The XANES spectrum of 0.5-Cr/DHS treated in such way (Fig. 4A, curve b) appeared then very similar to that reported in literature for a Cr^{2+}/SiO_2 Phillips catalyst having the same Cr loading.[34, 36, 41, 42] In particular: i) the edge is downward shifted (6002 eV) with respect to the oxidized sample, testifying that the treatment in CO caused a reduction of Cr^{6+} sites; ii) two weak pre-edge features are observed at 5988 and 5990 eV, due to Cr1s → (Cr3d + O2p) dipole-forbidden transitions;[31, 41, 42] iii) an intense and well resolved pre-edge peak is observed at 5994.2 eV, assigned to a Cr1s → Cr4p transition and considered the fingerprint of isolated Cr^{2+} sites.[31, 41, 42] Hence, in the following the XANES spectrum of 0.5-Cr/DHS treated in CO at 623 K will be considered as representative of isolated, highly uncoordinated, Cr^{2+} sites. Accordingly, the corresponding DR UV-Vis-NIR spectrum (Fig. 4B, curve b) did not longer contain any trace of the band at 21500 cm^{-1} characteristic of chromate species. The spectrum is dominated by intense bands at ca. 41000 and 30500 cm^{-1}, due to $O^{2-} \rightarrow Cr^{2+}$ charge transfer transitions,[29, 34, 40] and show two very weak signals at ca. 12500 and 7000 cm^{-1}, due to Cr^{2+} d-d transitions typical for Cr^{2+} ions in (pseudo)tetrahedral coordination.[34, 41]

The same evolution occurred for the DR UV-VIS-NIR spectra of all other samples (Fig. S4 in the ESI). In summary, XANES and DR UV-Vis-NIR data provided evidence that all the Cr/DHS catalysts contained well dispersed and fully accessible Cr species, which can contribute to the functional behaviour of the catalysts.

3.3. Brønsted and Lewis surface acidity

The assessment of the presence of Brønsted acid sites is of interest in the elucidation of the surface properties of catalysts used for paraffin dehydrogenation, because such centres can promote the transformation of the produced olefins in carbonaceous species,[43] finally responsible for reversible deactivation by coking.

IR spectra of NH_3 dosed onto the dehydr/ox catalysts were then recorded. The whole set of data is reported in Fig. S5 in the ESI, while here, only the result of their quantitative analysis is reported, for the sake of brevity. Briefly, other than bands due to ammonia molecules in interaction with silanols and Cr^{6+} centres (acting as

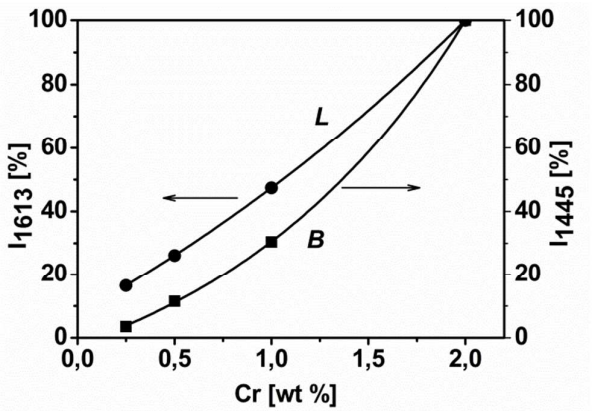

Fig. 5. Relative integrated intensity of the IR absorption bands NH_3 adsorbed on Cr/DHS samples, due to Lewis (L, band at 1613 cm^{-1}) and Brønsted (B, band at 1445 cm^{-1}) acidity vs. chromium content. Original spectral data in Fig. S5A in the ESI.

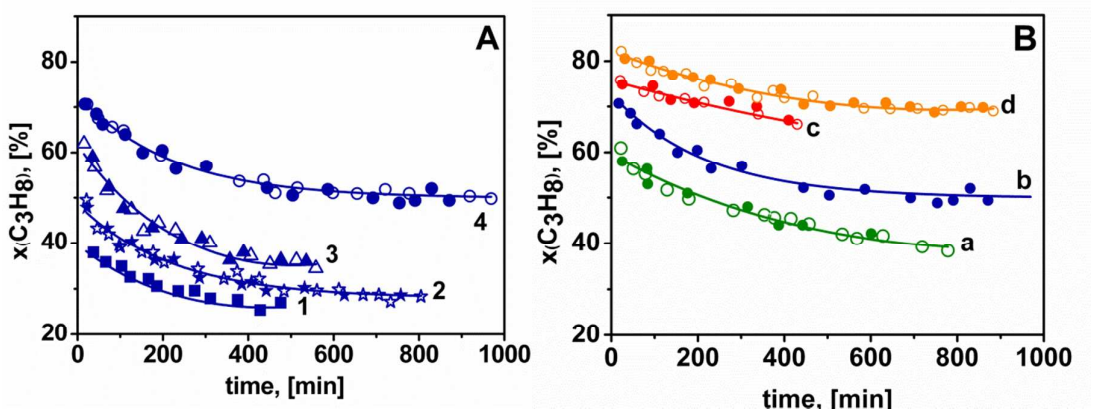

Fig. 6. C_3H_8 conversion vs. reaction time during ODH of propane on the Cr/DHS catalysts (T= 873 K, w= 200 h^{-1}) in the as-prepared state (open symbols) and after reaction and subsequent treatment in flowing O_2 at 873 K for 6h (full symbols: after 5-8 runs). Part A refers to reaction performed using CO_2 as oxidant (C_3H_8:CO_2:N_2=15:30:55) on the catalyst: 1) 0.25-Cr/DHS, 2) 0.5-Cr/DHS, 3) 1.0-Cr/DHS, 4) 2.0-Cr/DHS. Part B shows data obtained on the 2.0-Cr/DHS catalyst in different reaction conditions: a) C_3H_8:N_2=15:85 (green curves; full symbols: after 5 runs); b) C_3H_8:CO_2:N_2=15:30:55 (blue curves; full symbols: after 8 runs); c) C_3H_8:O_2:N_2=15:3:82 (red curves; full symbols: after 5 runs); d) C_3H_8:CO_2:O_2:N_2=15:30:3:52 (orange curves; full symbols: after 8 runs).

Lewis acid sites), signals typical of ammomium species were also detected, except for the bare MCM-41 silica, as expected. The formation of ammonium ions clearly monitored the occurrence of proton transfer from surface Brønsted acid centers, as reported also for other Cr-MCM-41 catalysts.[25] This kind of surface sites were also found to appear, with respect to the bare silica supports, as a consequence of the dispersion on SiO_2 of Ti^{4+},[44] and V^{5+},[45-47] ions. However, an explanation for their appearance has not been provided yet.

The spectra were normalized to both the optical thickness (see Fig. S4A and related comments) and SSA_{BET} of the samples, and then differences in the integrated intensity of the IR bands among the various catalysts became dependent only on differences in the amount of surface sites adsorbing ammonia. On such a basis, the integrated area of signals typical for NH_3 molecules probing Lewis acid sites (i.e. Cr^{6+} centres) and for NH_4^+ species, monitoring the presence of Brønsted acid sites, were plotted against the Cr content of the catalysts (Fig. 5). An almost linear relationship was obtained in the case of probe molecules on Lewis acid sites, whilst a concave trend appeared in the case of ammonium species, indicating that the formation of Brønsted acid sites was favored at high Cr loading (Fig. 5).

3.4. Catalytic tests

3.4.1. Effect of the Cr content in ODH of C_3H_8 using CO_2 as oxidant

One of the main targets of this work was to test the resistance of the catalysts towards irreversible deactivation under demanding reaction conditions. To this aim, the catalysts were fed with inlets at very low space velocity (200 h^{-1}) for ca. 15 hours, then re-activated

Table 2. ODH of propane on Cr/DHS catalysts prepared by "one-pot" method: Initial propane and carbon dioxide conversion (x), selectivity toward formed hydrocarbons (S) and yield of olefins (Y) , T=600°C, w=200h-1.

entry	Cr, %	$x_{C_3H_8}$, %	x_{CO_2}, %	$S_{C_2H_6}$, %	$S_{C_2H_4}$, %	$S_{C_2H_6}$, %	$S^*_{CH_4}$, %	$Y_{C_2H_6}$, %	$Y_{C_2H_4+C_2H_6}$, %
Part A: C_3H_8:CO_2:N_2=15:30:55, after 20 min of the reaction									
1	0.25	38	4	81	11	7	0	31	35
2	0.5	50	9	75	9	8	0.5	37	41
3	1.0	62	16	73	8	8	2.8	45	50
4	2.0	71	19	63	7	13	2.5	47	50
Part B*: C_3H_8:CO_2: O_2:N_2 =15:30:3:52, after 20 min of the reaction									
5	0.25	57	-	56	19	11	0.3	32	43
6	0.5	70	-	53	18	15	1.2	37	50
7	1.0	77	-	46	18	9	3.6	35	49
8	2.0	82	-	43	18	14	7.3	35	50

* - selectivity to the "excess" methane, i.e. methane formed in the process of ethane cracking, as methane was formed in the cracking of both propane (1:1) and ethane (1:2).

** - the sum of all selectivities was never equal to 100%, as C atoms were also involved in the formation of coke. At the beginning of the process ∑SC3+C2+C1 for 2.0-Cr/DHS was ca. 80% and only after ca.10 h it approached to 100%, due to the stabilization of the coke formation, accompanied with a significant the increase of propene selectivity and some decrease in the activity of the cracking processes.

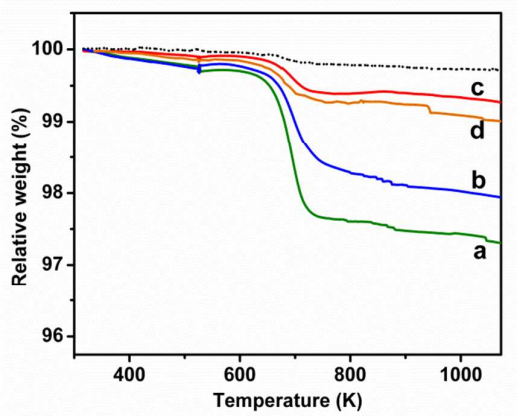

Fig. 7. Thermogravimetric analysis of the amount of coke formed on the 2.0-Cr/DHS catalyst after 400 min of ODH of propane reaction (T=873 K, w=200h^{-1}) in different conditions: a) C_3H_8:N_2=15:85 (green); b) C_3H_8:CO_2:N_2=15:30:55 (blue); c) C_3H_8:O_2:N_2=15:3:82 (red); d) C_3H_8:CO_2:O_2:N_2=15:30:3:52 (orange).

in air at 873 K for at least 6 h and employed in a subsequent series of 5-8 catalytic runs. The results are reported in Fig. 6 in terms of propane conversion. Panel A shows the data obtained for all catalysts by using CO_2 alone as oxidant; whereas panel B displays data obtained for 2.0-Cr/DHS (exhibiting the best performance in the test reported in panel A) but using different oxidative conditions (CO_2, O_2, CO_2+O_2), and also without any oxidant (direct dehydrogenation).

Moreover, all other catalysts were tested by using the CO_2+O_2 oxidant mixture, and the results obtained are reported in Fig. S6 in the ESI.

Focussing on data in panel A, it can be observed that initial C_3H_8 conversion in ODH with CO_2 as oxidant increased from ca. 40% for 0.25-Cr/DHS to ca. 70% for 2.0-Cr/DHS (curves 1-4). Thermodynamic calculations indicated that the equilibrium conversion of propane in the reaction $C_3H_8 + CO_2 = C_3H_6 + CO + H_2O$ carried out at 873 K is ca. 67%.[20] However, it must be considered that parallel reactions also contributed to C_3H_8 conversion. Actually, some H_2 (< 0.5 mol%) was found among the products when CO_2 alone was used as oxidant, likely resulting for the occurrence to some extent of both propane direct dehydrogenation and water gas shift reaction. By increasing the reaction time, propane conversion decreased, monitoring the occurrence of some catalyst deactivation, but it remained as high as ca. 50% in the case of 2.0-Cr/DHS (curve 4). However, the coincidence between the behaviour exhibited by each catalyst in the first (open symbols) and subsequent (full symbols) 5-8 runs, is a clear evidence that no irreversible deactivation occurred. In fact, DR UV-Vis-NIR spectra of catalysts after the first run and then treated in flowing O_2 at 873 K appeared almost coincident (and then not shown) to those recorded for the fresh form (Fig. S3 in the ESI), monitoring the invariance of the speciation of surface chromium after the reactivation treatment subsequent catalytic runs.

The observed decrease in propane conversion should be attributed to coke formation, that affected in a different way the activity of the various catalysts, likely resulting from the combination of different textural features (e.g., porous structures could be more easily blocked by coke) and different amount of Brønsted acid sites (increasing as the Cr content increased), as well as reversible changes in the speciation of supported Cr species (see below).

Details on the initial performances of the catalysts are listed in Table 2. Yields in both C_3H_6 and total olefins (just + 3-5%) exhibited a similar trend by increasing the Cr loading, indicating that basic and side reactions were affected in a similar way by this parameter. It is noteworthy that in the case of 2.0-Cr/DHS Y_{C3H6} of ca. 47% was attained using CO_2 as oxidant, which is significantly higher than the performance of the best catalyst reviewed by Cavani et al..[2]. Moreover, such initial Y_{C3H6} corresponded to those obtained by Chen et al. for GaO_x based materials,[4] and by Ovsitser et al. for VOx supported catalysts.[6] In addition, we confirmed the repeatability of these performances over several reaction runs. The mass balance for C, H and O was calculated for each point of each run. A maximum discrepancy of ca. 7 % was obtained only for C and ascribed to coke formation.

3.4.2 Effect of the type(s) of oxidant

To clear up the role of oxidants, the 2.0-Cr/DHS catalyst, which exhibited the best propane ODH performances in the presence of CO_2, was tested also using O_2 and CO_2+O_2mixture as oxidant, as well as in direct dehydrogenation conditions (Fig. 6B). Noticeably, no irreversible deactivation occurred, independently on the dehydrogenation conditions, as indicated by the overlapping of the propane conversion curves obtained for subsequent catalytic runs. The catalyst appeared quite active also in propane direct hydrogenation (curve a), but both the initial and final C_3H_8 conversion (ca. 60% and 40%, respectively) resulted significantly lower than for the tests carried out in ODH conditions (curves b-d). Besides differences in direct or oxidative dehydrogenation mechanisms,[48, 49] it might be considered that in the presence of oxidants an extra withdrawal of H_2 resulting by still occurring direct dehydrogenation can take place, then favoring also this C_3H_8 conversion route.[50, 51] As a result of the different mechanisms and other possible simultaneous beneficial effect, the initial C_3H_8 conversion values obtained for ODH in the presence of CO_2, O_2 or CO_2+O_2 were of ca. 70, 75 an 80%, in the order, which decreased to ca. 50, 65 and 70% after 900 min of reaction (value extrapolated for ODH with O_2). The combination of these factors appeared more effective when O_2 instead of CO_2 was used as oxidant (curves c and b, respectively). When only O_2 was used as oxidant, small amounts of CO and CO_2 (yield of ca. 3% for both) were also detected. However, even higher C_3H_8 conversion and catalyst stability were attained using the CO_2+O_2 mixture (curve d).

Of course, the switch from direct to oxidative propane dehydrogenation was expected to affect also the formation of coke.

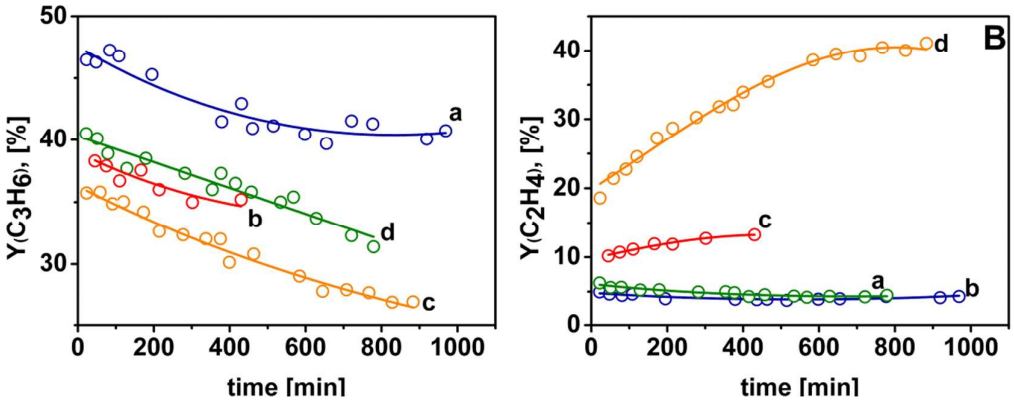

Fig. 8. Yields of C_3H_6 (panel A) and C_2H_4 (panel B) vs. reaction time during ODH of propane on the 2.0-Cr/DHS catalyst (T=873 K, w=200 h^{-1}) in different reaction conditions: a) C_3H_8:N_2=15:85 (green); b) C_3H_8:CO_2:N_2=15:30:55 (blue); c) C_3H_8:O_2:N_2=15:3:82 (red); d) C_3H_8:CO_2:O_2:N_2=15:30:3:52 (orange).

Accordingly, TGA data (Fig. 7) indicated that the weight loss assignable to coke removal by heating in air decreased from ca. 3 wt% for the catalyst tested in direct hydrogenation (curve a) to ca. 2 wt% when it was used for ODH in the presence of CO_2 (curve b), and to ca. 1-0.5 wt% when the oxidant for ODH was O_2 or the O_2+CO_2 mixture (curves c,d, respectively). **yield**

3.4.3 Olefin yield

By combining propane conversions obtained with 2.0-Cr/DHS catalyst in the various reaction conditions with selectivity toward propylene and total olefins (reported in Fig. S7 in ESI), C_3H_6 and C_2H_4 yields were calculated (Fig. 8, panel A and B, respectively).

The most important result is represented by the yield in the two olefins resulting from ODH in the presence of CO_2 as oxidant (panel A, curve b): the initial C_3H_6 yield was of ca. 47% (see also Table 2 and related comment), and remained as high as ca. 40% after 1000 min of reaction. Noticeably, these performances were reproduced after each catalyst regeneration. At the best of our knowledge, this C_3H_6 yield for propane ODH processes on Cr/SiO_2 catalyst operated for such a long time is equivalent to what reported for ODH of propane on VO_x/SiO_2 catalysts.[6] Moreover, the C_2H_4 yield remained quite low (Y≤ 5%) along the all duration of the test (panel B, curve b), suggesting that propane ODH with CO_2 as oxidant on Cr/SiO_2 catalysts can be of actual interest for the production of C_2 and C_3 olefins mixture highly rich in C_3H_6.

Also direct dehydrogenation resulted in a quite low (and constant) yield in ethene (Y≤ 5%, panel B, curve a), but accompanied by yield in C_3H_6 significantly lower than in the previous case, ranging from ca. 40 down to ca. 32% (panel A, curve a). Passing to ODH processes carried out using O_2, or O_2+CO_2, even lower C_3H_6 yields were obtained (panel A, curves c and d). However, in these cases accompanied by higher C_2H_4 yields, which in the case of ODH with O_2+CO_2 as oxidant became the main product after ca.300 min of reaction (panel B, curves B and C). The higher production of C_2H_4 might be the results of the enhanced cracking of propane in the presence of O_2,[52] also responsible for the production of larger excess of CH_4 (reported in Fig.S8 in the ESI). Hence, the results obtained in propane ODH using O_2 or O_2+CO_2 suggest that it could be worthwhile to investigate the possibility to tune the O_2/CO_2 ratio in order to obtain a desired composition of the olefin mixture to obtain tailored feeds for C_2H_4/C_3H_6 copolymerization.

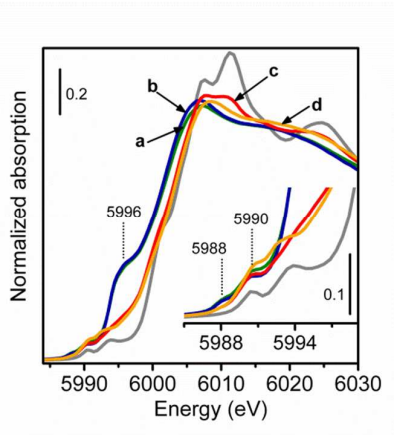

Fig. 9 Normalized XANES spectra of 1.0-Cr/DHS sample after treatment in different propane dehydrogenation reaction conditions: a) only C_3H_8 (green curve), b) C_3H_8+CO_2 (blue curve), c) C_3H_8+O_2 (red curve) and d) C_3H_8+CO_2+O_2 (orange curve). Spectrum of Cr_2O_3 is shown as reference for comparison (grey curve).

3.4.4 Effect of different oxidants on the oxidation state and dispersion of Cr sites

XANES spectroscopy is an atomic selective technique, and then allowed to monitor the actual oxidation state of chromium sites even in presence of coke. On such a basis, aliquots of the 1.0-Cr/DHS catalysts were treated in the presence of the various reaction mixtures *in situ* in the cell used for XANES measurements. The selection of the 1.0-Cr/DHS catalyst resulted from sample availability and Cr content high enough to obtain XANES spectra with a satisfactory signal to noise ratio in the presence of

carbonaceous deposits, resulting in a further dilution of Cr content. However, the results of the characterization activity reported above (section 3.2) indicated that the speciation of Cr can be considered equivalent for all catalysts.

Fig. 9 shows the XANES spectra of 1.0-Cr/DHS samples treated in the various model reaction conditions, compared with the spectral profile of Cr_2O_3 as reference compound (grey curve).

The data can be straightforwardly divided in two groups. One is constituted by the spectra of the catalysts used in direct dehydrogenation and in ODH with CO_2 as oxidant (curves a and b): both spectra have the edge (evaluated at the maximum of the derivative curve) at 6002 eV, accompanied by an intense and broad pre-edge peak centred around 5996 eV, and by two weak pre-edge peaks at 5988 and 5990 eV. All these signals witness for the presence of Cr^{2+} species, as previously discussed for 0.5-Cr/DHS reduced in CO (Fig. 4A, curve b). The higher intensity of the white line feature suggests that the Cr^{2+} sites obtained during propane ODH reaction have a higher number of ligands.

Conversely, the spectra of the catalyst used for ODH with O_2 or O_2+CO_2 as oxidant (curves c and d) exhibited a double edge at higher energy (5999 and 6003 eV) and two weak pre-edge peaks 5990 and 5993 eV. These three features appeared very similar to those present in the spectrum of Cr_2O_3 reference compound. Moreover, the spectrum of the catalyst used for ODH with O_2+CO_2 as oxidant was characterized, in the white-line region, by a weak, ill resolved doublet at 6008 and 6010 eV, which can result from multiple-scattering contributions of Cr_2O_3-like particles. The aggregation of Cr species under reaction condition was proposed to occur in propane ODH with O_2 as oxidant,[16] then reversed by subsequent catalyst reactivation in oxygen.

Thereby, the in situ XANES measurements provided evidence that during direct dehydrogenation or ODH in the presence of CO_2 the active chromium species are in average in the +2 oxidation state, whereas when O_2 was used for ODH (alone or mixed with CO_2) their average oxidation state should be +3.

Conclusions

The DHS method can be successfully employed to obtain Cr/SiO_2 catalysts with high specific surface area and a texture characterized by the co-presence of ordered mesoporous, disordered mesoporous and non-porous particles, their relative amount depending on the Cr content. However, (ordered) porosity did not appear a requisite to have highly active catalysts. All chromium was present as highly dispersed surface chromate species, and the amount of Cr sites (evaluated in terms of their behaviour as Lewis acid centres towards NH_3) was found linearly proportional to the Cr loading. The formation of surface chromate species was accompanied by the appearance of Brønsted acid sites, relatively more abundant for higher Cr contents.

All the investigated catalysts appeared stable towards possible irreversible deactivation in the ODH of propane, in reaction conditions as close as possible to industrial applications, and allowed the attainment of yields in propene (and total olefins) among the highest reported in the literature, in particular by using CO_2 alone as oxidant, where YC_3H_6 still remained as high as 40% after 1000 min of reaction at very low space velocity, in order to attain conversion of industrial interest.

Finally, XANES data of reacted catalyst indicated that when CO_2 is used as oxidant in ODH, the average oxidation state of Cr sites can be as low as +2, whereas it can be as low as 3+ in the presence of (also) O_2 as oxidant. It seems reasonable to propose that thise possible difference in oxidation state of Cr sites might contribute to the origin of differences in selectivity, and then yield, in C_3H_6 and C_2H_4 in dependence on the oxidation agent.

Acknowledgements

Authors are grateful to Olivier Mathon (BM23 at ESRF) and to Giovanni Agostini and Caterina Barzan for the friendly assistance during the XAS experiments. University of Torino and Compagnia di San Paolo (project ORTO11RRT5) and RFBF-ASP (grant N. 07-03-951581) are acknowledged for funding.

References

1. http://pubs.acs.org/cen/coverstory/83/8312 petrochemicals.html.
2. F. Cavani, N. Ballarini and A. Cericola, *Catalysis Today*, 2007, **127**, 113-131.
3. J. J. H. B. Sattler, J. Ruiz-Martinez, E. Santillan-Jimenez and B. M. Weckhuysen, *Chemical Reviews*, 2014, **114**, 10613-10653.
4. M. Chen, J. Xu, F. Z. Su, Y. M. Liu, Y. Cao, H. Y. He and K. N. Fan, *Journal of Catalysis*, 2008, **256**, 293-300.
5. C. A. Carrero, R. Schloegl, I. E. Wachs and R. Schomaecker, *ACS Catalysis*, 2014, **4**, 3357-3380.
6. O. Ovsitser, R. Schomaecker, E. V. Kondratenko, T. Wolfram and A. Trunschke, *Catalysis Today*, 2012, **192**, 16-19.
7. O. Ovsitser and E. V. Kondratenko, *Chemical Communications*, 2010, **46**, 4974-4976.
8. F. A. F. Frusteri, G. Calogero, T. Torre, A. Parmaliana, *Catalysis Communications*, 2001, **2**, 49-56.
9. A. I. Tsyganok, T. Tsunoda, S. Hamakawa, K. Suzuki, K. Takehira and T. Hayakawa, *Journal of Catalysis*, 2003, **213**, 191-203.
10. Y. Wang, Q. L. Zhuang, Y. Takahashi and Y. Ohtsuka, *Catalysis Letters*, 1998, **56**, 203-206.
11. H. L. Wan, X. P. Zhou, W. Z. Weng, R. Q. Long, Z. S. Chao, W. D. Zhang, M. S. Chen, J. Z. Luo and S. Q. Zhou, *Catalysis Today*, 1999, **51**, 161-175.
12. N. Mimura, M. Okamoto, H. Yamashita, S. T. Oyama and K. Murata, *Journal of Physical Chemistry B*, 2006, **110**, 21764-21770.
13. Y. Ohishi, T. Kawabata, T. Shishido, K. Takaki, Q. H. Zhang, Y. Wang and K. Takehira, *Journal of Molecular Catalysis A: Chemical*, 2005, **230**, 49-58.
14. J. Santamaria-Gonzalez, J. Merida-Robles, M. Alcantara-Rodriguez, P. Maireles-Torres, E. Rodriguez-Castellon and A. Jimenez-Lopez, *Catalysis Letters*, 2000, **64**, 209-214.
15. I. Takahara and M. Saito, *Chemistry Letters*, 1996, 25, 973-974.
16. K. Takehira, Y. Ohishi, T. Shishido, T. Kawabata, K. Takaki, Q. H. Zhang and Y. Wang, *Journal of Catalysis*, 2004, **224**, 404-416.
17. S. B. Wang, K. Murata, T. Hayakawa, S. Hamakawa and K. Suzuki, *Applied Catalysis A: General*, 2000, **196**, 1-8.

18. Y. Wang, Y. Ohishi, T. Shishido, Q. H. Zhang, W. Yang, Q. Guo, H. L. Wan and K. Takehira, *Journal of Catalysis*, 2003, **220**, 347-357.
19. H. Yang, S. L. Liu, L. Y. Xu, S. J. Xie, Q. X. Wang and L. W. Lin, *Natural Gas Conversion VII*, 2004, **147**, 697-702.
20. M. A. Botavina, G. Martra, Y. A. Agafonov, N. A. Gaidai, N. V. Nekrasov, D. V. Trushin, S. Coluccia and A. L. Lapidus, *Applied Catalysis A: General*, 2008, **347**, 126-132.
21. V. C. Corberán, *Catalysisl Today*, 2005, **99**, 33-41.
22. T. Kamegawa, J. Morishima, M. Matsuoka, J. M. Thomas and M. Anpo, *Journal of Physical Chemistry C*, 2007, **111**, 1076-1078.
23. H. L. L. Liu, Y. Zhang, *Catalysis Communications*, 2007, **8**, 565-570.
24. S. C. Laha and R. Glaser, *Microporous and Mesoporous Materials*, 2007, **99**, 159-166.
25. M. Lezanska, G. S. Szymanski, P. Pietrzyk, Z. Sojka and J. A. Lercher, *Journal of Physical Chemistry C*, 2007, **111**, 1830-1839.
26. C. S. S. Shylesh, A.P. Singh, B.G. Anderson *Microporous and Mesoporous Materials*, 2007, **99**, 334-344.
27. S. H. Shen and L. J. Guo, *Catal Today*, 2007, **129**, 414-420.
28. C. Subrahmanyam, B. Louis, F. Rainone, B. Viswanathan, A. Renken and T. K. Varadarajan, *Applied Catalysis A: General*, 2003, **241**, 205-215.
29. E. G. A. Zecchina, G. Ghiottl, C. Morterra, E. Borello *The Journal of Physical Chemistry*, 1975, **79**, 966-972.
30. S. Samanta, N. K. Mal and A. Bhaumik, *Journal of Molecular Catalysis A: Chemical*, 2005, **236**, 7-11.
31. S. Bordiga, E. Groppo, G. Agostini, J. A. van Bokhoven and C. Lamberti, *Chemical Reviews*, 2013, **113**, 1736-1850.
32. C. A. Demmelmaier, R. E. White, J. A. van Bokhoven and S. L. Scott, *Journal of Catalysis*, 2009, **262**, 44-56.
33. C. A. Demmelmaier, R. E. White, J. A. van Bokhoven and S. L. Scott, *Journal of Physical Chemistry C*, 2008, **112**, 6439-6449.
34. E. Groppo, C. Lamberti, S. Bordiga, G. Spoto and A. Zecchina, *Chemical Reviews*, 2005, **105**, 115-183.
35. E. Groppo, C. Prestipino, F. Cesano, F. Bonino, S. Bordiga, C. Lamberti, P. C. Thune, J. W. Niemantsverdriet and A. Zecchina, *Journal of Catalysis*, 2005, **230**, 98-108.
36. B. M. Weckhuysen, R. A. Schoonheydt, J. M. Jehng, I. E. Wachs, S. J. Cho, R. Ryoo, S. Kijlstra and E. Poels, *Journal of the Chemical Society-Faraday Transactions*, 1995, **91**, 3245-3253.
37. B. M. Weckhuysen, A. A. Verberckmoes, A. L. Buttiens and R. A. Schoonheydt, *Journal of Physical Chemistry*, 1994, **98**, 579-584.
38. R. L. Puurunen, B. G. Beheydt and B. M. Weckhuysen, *Journal of Catalysis*, 2001, **204**, 253-257.
39. B. M. Weckhuysen, I. E. Wachs and R. A. Schoonheydt, *Preparation of Catalysts Vi*, 1995, **91**, 151-158.
40. B. M. Weckhuysen, I. E. Wachs and R. A. Schoonheydt, *Chemical Reviews*, 1996, **96**, 3327-3349.
41. D. Gianolio, E. Groppo, J. G. Vitillo, A. Damin, S. Bordiga, A. Zecchina and C. Lamberti, *Chemical Communications*, 2010, **46**, 976-978.
42. E. Groppo, K. Seenivasan and C. Barzan, *Catalysis Science & Technology*, 2013, **3**, 858-878.
43. G. Bellussi, G. Centi, S. Perathoner and F. Trifiro, *Catalytic Selective Oxidation*, 1993, **523**, 281-297.
44. Y. Hu, S. Higashimoto, G. Martra, J. L. Zhang, M. Matsuoka, S. Coluccia and M. Anpo, *Catalysis Letters*, 2003, **90**, 161-163.
45. G. Busca, L. Marchetti, G. Centi and F. Trifiro, *Journal of the Chemical Society-Faraday Transactions I*, 1985, **81**, 1003-1014.
46. G. Martra, F. Arena, S. Coluccia, F. Frusteri and A. Parmaliana, *Catalysis Today*, 2000, **63**, 197-207.
47. H. Miyata, K. Fujii and T. Ono, *Journal of the Chemical Society-Faraday Transactions I*, 1988, **84**, 3121-3128.
48. O. F. Gorriz and L. E. Cadus, *Applied Catalysis A: General*, 1999, **180**, 247-260.
49. B. M. Weckhuysen and R. A. Schoonheydt, *Catalysis Today*, 1999, **51**, 223-232.
50. K. Nakagawa, C. Kajita, N. Ikenaga, M. Nishitani-Gamo, T. Ando and T. Suzuki, *Catalysis Today*, 2003, **84**, 149-157.
51. L. Y. Xu, J. X. Liu, Y. D. Xu, H. Yang, Q. X. Wang and L. W. Lin, *Applied Catalysis A: General*, 2000, **193**, 95-101.
52. V. R. Choudhary, V. H. Rane and A. M. Rajput, *AIChE Journal*, 1998, **44**, 2293-2301.

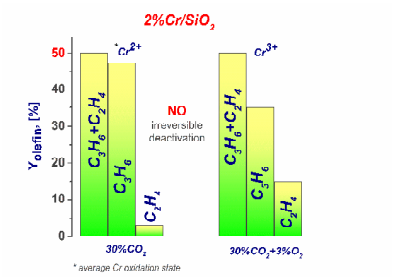

CrO_x/SiO_2 catalysts with high propene/olefin yield, stable towards irreversible deactivation, are proposed for oxidative dehydrogenation of propane with CO_2